Nanotechnology **20** (2009) 095502 (5pp) doi:10.1088/0957-4484/20/9/095502

# A multi-walled carbon nanotube–aluminum bimorph nanoactuator

**Onejae Sul and Eui-Hyeok Yang**[1]

Mechanical Engineering Department, Stevens Institute of Technology, Castle Point on Hudson, Hoboken, NJ 07030, USA

E-mail: eyang@stevens.edu

Received 27 October 2008, in final form 21 January 2009
Published 11 February 2009
Online at stacks.iop.org/Nano/20/095502

**Abstract**

A multi-walled carbon nanotube (MWNT) bimorph nanoactuator has been modeled, fabricated and characterized. A thin aluminum film was uniformly deposited on the sidewalls of MWNTs using a pulsed laser deposition method to create the bimorph nanostructure. For a temperature change from 290 to 690 K with measured dimensions of $100 \pm 20$ nm for the MWNT diameter, $40 \pm 10$ nm for the Al thickness, and $5.2 \pm 0.5$ $\mu$m for the bimorph length, the measured deflection was $550 \pm 200$ nm, which was in good agreement with the calculation. The actuation force was measured using a lateral force microscopy technique, and the measured values agreed well with the prediction based on the model. The nanoactuator generated a $\mu$N force at its tip.

(Some figures in this article are in colour only in the electronic version)

## 1. Introduction

Manipulation of nanoscale objects has been accomplished using surface probe microscope (SPM) systems or nanotweezer systems [1–4]. However, measurement of nano-newton level force generated by individual actuators is much more complicated and thus requires further research [5–9]. Research on microactuators using thermal stress as the driving mechanism has been very active, because of the relatively large amount of force generated from simple device structures [10]. In addition, applications of such microactuators, including mirrors [11–13, 10], conveyer systems [14, 15], tweezers [16–19] and ciliary systems [20, 21] and fixtures [22] were reported. To further reduce the size of actuators, a nanotweezer—a pair of nanotubes attached at the end of a glass rod, which was capable of picking up microparticles was studied [23]. A nanoscale trimorph device (metal oxide–multiwall carbon nanotube (MWNT)–metal oxide) was developed for thermal actuation based on MWNTs by depositing two thin metal-oxide films on opposing sidewalls of a MWNT [24]. Upon heating the body of the MWNT, the structure achieved thermal deflection as a result of the mismatch of coefficients of thermal expansion (CTE) between two different metal oxides. However, there are remaining issues of (1) fabrication of a nanoactuator structure using MWNT as a bimorph layer, but not as a template, in order to create the device in a much simpler way, and (2) direct force measurement from nanoactuators, which is not yet reported. The fabrication of 'bimorph' is beneficial, since the CTE of MWNT (less than $3 \times 10^{-6}$ K$^{-1}$) [25] is much smaller than that of Al ($23 \times 10^{-6}$ K$^{-1}$) in the temperature range of up to 550 K. To create nanoscale bimorph structures, the key fabrication issue is the deposition of a metal film on only one side of a MWNT exposing the other side as a bare MWNT surface, requiring a directional deposition method. Further, the measurement of minuscule force generated from nanoactuators is required.

In our study, a thermal actuation approach using MWNT–Al bimorph is chosen for two reasons. First, a CNT bimorph can act as a very sturdy nanolayer under repeated bending, and MWNTs in particular are well known for mechanical resilience under extreme bending [26]. Typically, MWNTs can be synthesized to be microns-long, thus, potentially allowing the deflection of one tip in the range of hundreds of nanometers. Second, thermal stress provides the largest stress in a wide range of scale. This will be advantageous in the fabrication of miniature actuator with a relatively large force generation. Bimorph nanostructures are currently being developed in the author's group using a pulsed laser deposition (PLD) system for precision film deposition on the sidewall of MWNTs. In this paper, the fabrication of MWNT bimorph nanoactuators and the characterization of the actuation force are presented. A transmission electron microscope (TEM) was used to assess

[1] Author to whom any correspondence should be addressed.

 

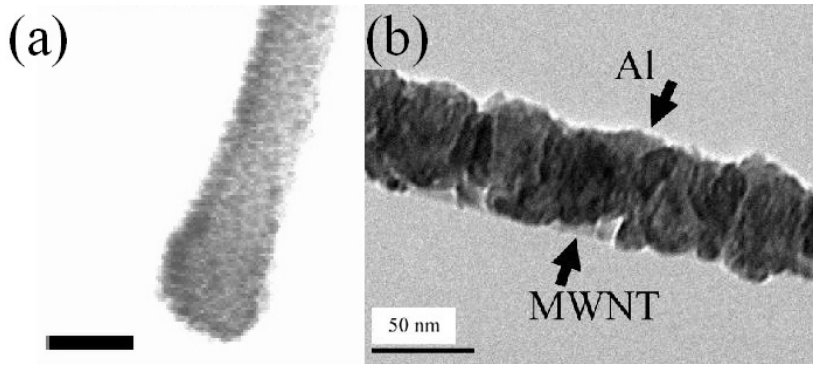


**Figure 1.** Nanoscale bimorph fabricated using a MWNT with a thermally evaporated Al film: (a) TEM image of an aluminum-covered MWNT by thermal evaporation without cooling. The scale bar is 20 nm. (b) TEM image of a MWNT with aluminum film on one side only. The aluminum was deposited at a low temperature stage, which was maintained at 150 K using liquid nitrogen inside the evaporator chamber. However, due to marginal uniform coverage of Al film, repeatable thermal deflections were not achieved.

the metal film quality, and a thermal stage was built inside an SEM chamber in order to test the thermal actuation capability of nanoactuators. The force generated from the nanoactuator was measured using a lateral atomic force microscopy (LFM) by applying an external counteracting load against its tip with an atomic force microscope (AFM) tip.

## 2. Fabrication

Chemical vapor deposition (CVD)-grown MWNTs (purchased from MER Corp.) were suspended by sodium dodecyl sulfate (SDS) in distilled water [27]. A droplet of the suspension containing the MWNTs was dispensed on silicon substrate. After dehydration, the substrate was broken into smaller pieces to find cantilevered MWNTs at substrate edges. Our initial attempt to create a bimorph nanostructure was by evaporation of Al on a MWNT cantilever by thermal evaporation at room temperature, where the metal atoms encapsulated the whole circumference of a MWNT due to the high kinetic energy of metal atoms (figure 1(a)). To fabricate the double layer by reducing this encapsulation, the sample stage was cooled down to 150 K using liquid nitrogen. However, formation of metal grains due to the now too low temperature still caused marginal Al film uniformity (figure 1(b)), hampering consistent actuation performance [10] (figure 1). In contrast, a PLD system allows deposition of Al on only one side of the MWNT with a precisely controlled thickness and uniformity [24], because of the low kinetic energy of ejected atoms from the target. In this experiment, a Nd:YAG (Quanta Ray, DCR2-10) laser was used to deposit Al, with a deposition rate of 0.6 Å $\text{min}^{-1}$ at 70 mJ/10 ns pulse. Figure 2(a) shows TEM images of a nanoactuator fabricated via the PLD deposition.

## 3. Modeling

If two layers of homogeneous materials, a and b, are stacked with thicknesses $d_a$, $d_b$, and modified Young's moduli $Y_a$, and $Y_b$, respectively, the resulting bimorph deflects at one end with a temperature variation $\Delta T$, by [28]

$$\Delta = \frac{3L^2(\alpha_{\text{Al}} - \alpha_{\text{MWNT}})\Delta T(d_{\text{Al}} - d_{\text{MWNT}})}{d_{\text{Al}}d_{\text{MWNT}}} \times \left[\left(\frac{d_{\text{Al}}}{d_{\text{MWNT}}}\right)^2 \frac{Y_{\text{Al}}}{Y_{\text{MWNT}}} + 4\frac{d_{\text{Al}}}{d_{\text{MWNT}}} + 6 + \left(\frac{d_{\text{MWNT}}}{d_{\text{Al}}}\right)^2 \frac{Y_{\text{MWNT}}}{Y_{\text{Al}}} + 4\frac{d_{\text{MWNT}}}{d_{\text{Al}}}\right]^{-1} \quad (1)$$

where $Y = E/(1-\nu)$, $E$ is Young's modulus, $\nu$ is Poisson ratio, and the $\alpha$s are thermal expansion rates, assuming a rectangular cross section for each layer. Young's modulus and coefficient of thermal expansion (CTE) of MWNT were obtained from [25, 29]. Thickness of each layer and the device length were measured using SEM and TEM. The reported CTE and Young's modulus were $3 \times 10^{-6}$ $\text{K}^{-1}$ [25] and 1 TPa [29] for MWNT, and $23 \times 10^{-6}$ $\text{K}^{-1}$ and 70 GPa for Al bulk values, respectively. Temperature of the sample substrate was measured using a thermocouple at the thermal stage inside the SEM. The bimorph tip generates a bending force against an external load at the tip. The amount of external load required to recover the bimorph to its room temperature geometry, is predicted by [28],

$$F = \frac{w(\alpha_{\text{Al}} - \alpha_{\text{MWNT}})\Delta T}{L} \times \frac{Y_{\text{Al}}Y_{\text{MWNT}}d_{\text{Al}}d_{\text{MWNT}}(d_{\text{Al}} + d_{\text{MWNT}})}{d_{\text{Al}}Y_{\text{Al}} + d_{\text{MWNT}}Y_{\text{MWNT}}} \quad (2)$$

where $w$ is width, which is identical to the diameter of the MWNT.

## 4. Thermal deflection and force measurements

For a temperature change from 290 to 690 K with measured dimensions of 100 ± 20 nm of MWNT diameter, 40 ± 10 nm of Al thickness, and bimorph length of 5.2 ± 0.5 $\mu$m (figures 2(b)–(d)), the deflection calculated was 430 nm using equation (1). The deflection measurement shown in figure 2(d) was 550 ± 200 nm, which was in good agreement with the calculation.

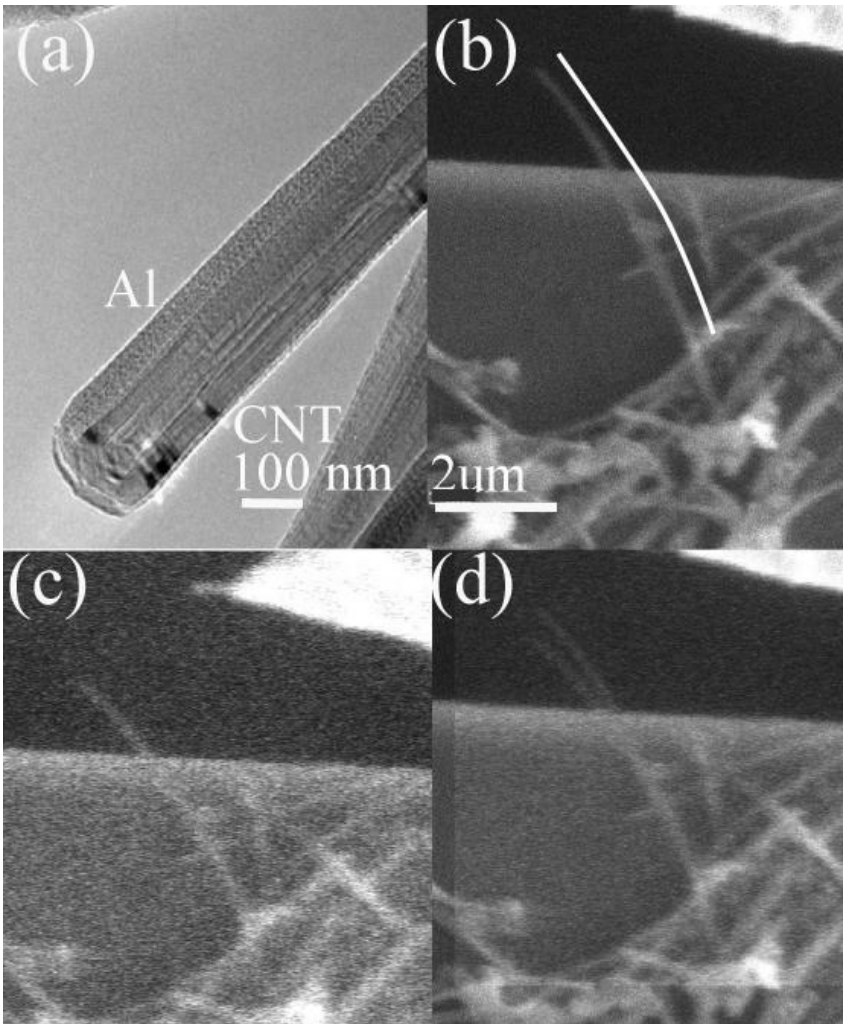


**Figure 2.** Nanoactuators fabricated using a MWNT with a uniform PLD-based Al film: (a) TEM image on MWNT–Al bimorph nanoactuators at a side view angle. (b) SEM image of a nanoactuator from the same PLD batch. A white line displays the entire length of the bimorph. The image was taken at 690 K in a thermal stage prepared inside the SEM. The thermal stage was used to control the substrate temperature. Al was deposited from left to right in the image. (c) SEM image taken at 290 K. (d) For comparison, the image (b) is superposed on the image (c).

The LFM technique was used to measure the actuation force generated from the nanoactuator. The force from the nanoactuator was measured by sweeping an AFM tip laterally at the middle of a bimorph (figure 3(a)). The thermally generated force twisted the AFM cantilever further, and this amount appeared as an increase as the temperature was elevated by a thermal stage under the AFM. The total force (reaction with thermal response) was calculated by $F = k_{\text{twist}} c_{\text{L}} I_{\text{L-R}}$, where $k_{\text{twist}}$ is torsion spring constant of an AFM cantilever, $c_{\text{L}}$ is a ratio between detected voltage versus AFM tip lateral swinging in nm mV$^{-1}$, and $I_{\text{L-R}}$ is the measured voltage in mV. $k_{\text{twist}}$ was calculated by $Et^3w/6(1+\nu)Lh^2$, where $E, L, t, w$, and $h$ are Young's modulus, length, thickness, width of the AFM cantilever, and height of the AFM tip (105 nN nm$^{-1}$). $c_{\text{L}}$ was calibrated by measuring the voltages generated at the quad-photodiode in the AFM, when the tip touched a step edge ($0.038 \pm 0.002$ nm mV$^{-1}$). The measured $I_{\text{L-R}}$ was used to calculate the amount of force applied at the AFM tip. Figure 3(b) shows the measurement results at 290 and 340 K from a bimorph with a 20 nm-thick Al film. The generated force from the nanoactuator was calculated by subtracting $I_{\text{L-R}}$ at the low temperature from the $I_{\text{L-R}}$ at the high temperature. The saw-tooth feature in $I_{\text{L-R}}$ implies the stick-slip when the AFM tip slides along the bimorph before release. This was also observed in a bare MWNT cantilever. The LFM measurement was repeated at $\Delta T = 0$ (298 K), 50, 100, 130, and at 0 K again. Figure 4 shows that the measured force agrees well with the prediction in equation (2).

## 5. Discussion

There is interest in studying the performance of nanoactuators, in terms of the maximum generated force divided by mass (i.e. force density). Ideally all types of biological or mechanical motors seek to produce large force with minimal mass. According to a study done on the universal scaling law on a force–mass relationship [30], our nanoactuator belongs to the linear type, which generates force through a linear stroke.

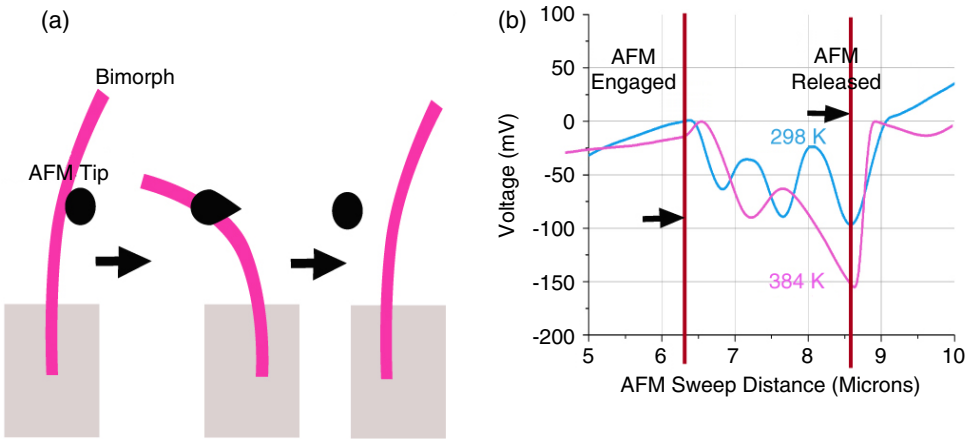


**Figure 3.** LFM-based force measurement results: (a) schematic on the force using LFM. The reaction force from the bimorph acting on the AFM tip generates an $I_{L-R}$ signal, like (b) as the AFM tip scans laterally, until the AFM tip is released. The thermal actuation force appears as an increase of $I_{L-R}$ signal at the higher temperature. (b) $I_{L-R}$ signal versus AFM scan distance at 290 and at 340 K.

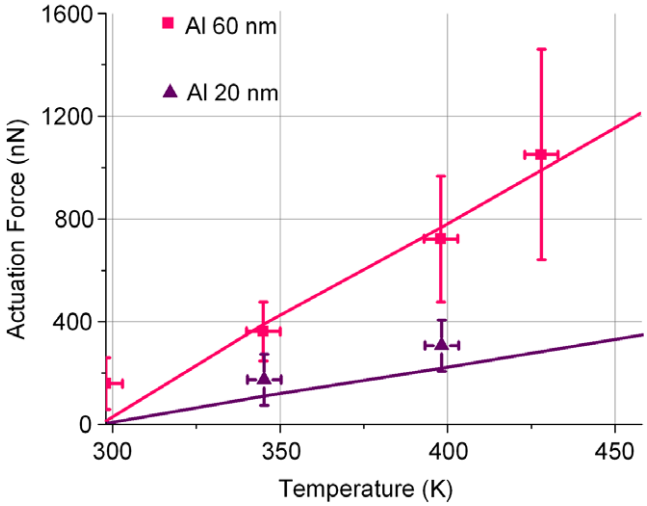


**Figure 4.** Temperature and thickness versus force. The lines represent the prediction from equation (2) based on the measured bimorph geometries. Al thickness was $60 \pm 10$ nm (red) and $20 \pm 5$ nm (purple), MWNT diameters were $200 \pm 20$ nm, and length of the bimorphs were $2.2 \pm 0.2$ $\mu$m. Room temperature measurement with 60 nm was done after cooling, indicating residual film stress. The error bars of the forces are either the standard deviation of multiple measurements or drift of $I_{L-R}$, where the larger value was chosen. In addition, the measurements were repeated three times at each temperature.

The governing equation of the law is force $= 887 \times (\text{mass})^{0.667}$. Following this equation, the expected force from the mass of the bimorph, $1.0 \times 10^{-16}$ kg, is only in the range of tens of nano-newtons. However, our equation (2) and measurements indicate that the maximum force can be in the range of $\mu$N depending on temperature variation, which is roughly one hundred times the expectation. This is much larger than average deviation (typically by a factor of 10) of individual motors from the law. The large force–mass ratio comes from the fact that the actuation force becomes larger when the length of the bimorph gets shorter at the cost of reduced deflections, which differs from other motors where large force is achieved by increase in mass. This advantage of relatively high force output can be used for the construction of light-weight motors, perhaps to be used as artificial muscle if multiple actuators are prepared.

## 6. Conclusions

MWNT–Al bimorph nanoactuators have been fabricated using a PLD technique. The bimorph nanostructure was verified using TEM, and the thermal actuation was measured and confirmed by thermal bending experiments inside an SEM. The actuation force generated at the tip of a nanoactuator was measured by scanning an AFM tip across it and simultaneously recording the AFM's twisting angle. The measured maximum force was approximately 1 $\mu$N at 430 K, which was in good agreement with the modeled prediction.

## Acknowledgments

The authors appreciate valuable advices and comments on the YAG laser by Professors Strauf and Whittaker in Department of Physics at Stevens Institute of Technology.

## References

[1] Falvo M R, Taylor R M II, Helser A, Chi V, Brooks F P Jr, Washburn S and Superfine R 1999 *Nature* **397** 236–8
[2] Molhave K, Hansen T M, Madsen D N and Boggild P 2004 *J. Nanosci. Nanotechnol.* **4** 279–82
[3] Tombler T W, Zhou C, Alexseyev L, Kong J, Dai H, Liu L, Jayanthi C S, Tang M and Wu S Y 2000 *Nature* **405** 769–72
[4] Hertel T, Martel R and Avouris P 1998 *J. Phys. Chem.* B **102** 910–5
[5] Kline T R, Paxton W F, Mallouk T E and Sen A 2005 *Angew. Chem. Int. Edn* **44** 744–6
[6] Kovalev A, Bauer G E W and Brataas A 2006 *Phys. Rev.* B **75** 01430–56
[7] Sul O, Falvo M R, Taylor R M II, Washburn S and Superfine R 2006 *Appl. Phys. Lett.* **89** 203512
[8] Dreyfus R, Baudry J, Roper M L, Fermigier M, Stone H A and Bibette J 2005 *Nature* **437** 862–5

[9] Donald B R, Levey C G, McGray C D, Rus D and Paprotny I 2006 *J. Microelectromech. Syst.* **15** 1–15
[10] Sul O 2006 *PhD Thesis* University of North Carolina at Chapel Hill
[11] Bernstein J J, Taylor W P, Brazzle J D, Corcoran C J, Kirkos G, Odhner J E, Pareek A, Waelti M and Zai M 2004 *J. Microelectromech. Syst.* **13** 526–35
[12] Van Kessel P F, Hornbeck L J, Meier R E and Douglass M R 1998 *Proc. IEEE* **86** 1687–704
[13] Jain A, Qu H, Todd S and Xie H 2005 *Sensors Actuators* A **122** 9–15
[14] Konishi S and Fujita H 1994 *J. Microelectromech. Syst.* **3** 54–8
[15] Suh J W, Glander S F, Darling R B, Storment C W and Kovacs G T A 1997 *Sensors Actuators* A **58** 51–60
[16] Nguyen N T, Ho S S and Low C L N 2004 *J. Micromech. Microeng.* **14** 969–74
[17] Luo J K *et al* 2005 *J. Micromech. Microeng.* **15** 1294–302
[18] Kim K *et al* 2004 *Microsyst. Technol.—Micro Nanosyst. Inform. Storage Process. Syst.* **10** 689–93
[19] Krulevitch P, Lee A P, Ramsey P B, Trevino J C, Hamilton J and Northrup M A 1996 *J. Microelectromech. Syst.* **5** 270–82
[20] Kladitis P E and Bright V M 2000 *Sensors Actuators* **80** 132–7
[21] Shu J W, Glander S F, Darling R B, Storment C W and Kovacs G T A 1997 *Sensors Actuators* A **58** 51–60
[22] Luo J K *et al* 2005 *J. Micromech. Microeng.* **15** 1406–13
[23] Kim P and Lieber C 1999 *Science* **286** 2148–50
[24] Ikuno T, Honda S, Yasuda T, Oura K, Katayama M, Lee J and Mori H 2005 *Appl. Phys. Lett.* **87** 213104
[25] Schelling P K and Keblinski P 2003 *Phys. Rev.* B **68** 035425
[26] Falvo M and Superfine R 2000 *J. Nanopart. Res.* **2** 237–48
[27] Lewenstein J C, Burgin T P, Ribayrol T P, Nagahara L A and Tsui R K 2002 *Nano Lett.* **2** 443–6
[28] Gehring G A, Cooke M D, Gregory I S, Karl W J and Watts R 2000 *Smart Mater. Struct.* **9** 918–31
[29] Treacy M M J, Ebbesen T W and Gibson J M 1996 *Nature* **381** 678–80
[30] Marden J H and Allen L R 2002 *Proc. Natl Acad. Sci.* **99** 4161–6